

# Compact 3D Microfluidic Channel Structures Embedded in Glass Fabricated by Femtosecond Laser Direct Writing

Changning Liu<sup>\*1</sup>, Yang Liao<sup>\*1</sup>, Fei He<sup>\*1</sup>, Jiangxin Song<sup>\*1</sup>, Di Lin<sup>\*1</sup>, Ya Cheng<sup>\*1†</sup>, Koji Sugioka<sup>\*2</sup>, Katsumi Midorikawa<sup>\*2</sup>

<sup>\*1</sup>State Key Laboratory of High Field Laser Physics, Shanghai Institute of Optics and Fine Mechanics, Chinese Academy of Sciences, P.O. Box 800-211, Shanghai 201800, China

<sup>\*2</sup>Laser Technology Laboratory, RIKEN - Advanced Science Institute, Hirosawa 2-1, Wako, Saitama 351-0198, Japan

†Email: ya.cheng@siom.ac.cn

We demonstrate rapid fabrication of complex three-dimensional (3D) microfluidic channels with lengths up to ~6.0 cm within a tiny volume down to ~80 nl in glass substrates by femtosecond laser direct writing, which, to the best of our knowledge, is the longest microfluidic channel directly embedded in glass by femtosecond laser microprocessing. The fabrication mainly includes the following two steps: (1) formation of hollow microfluidic channels in porous glass by scanning a tightly focused femtosecond laser beam inside a porous glass immersed in water; and (2) postannealing of the fabricated porous glass sample at ~1150 °C for consolidation of the sample. The unique 3D capability of our technique allows construction of extremely compact microfluidic devices and systems.

DOI:10.2961/jlmn.2013.02.0010

**Key words:** femtosecond laser micromachining, three-dimensional, microfluidic channel

## 1. Introduction

Microfluidics is a burgeoning field with important application in many areas of research, such as chemical synthesis, biotechnology and optofluidic technology. By integrating fluidic functions including metering, mixing, valving, transport, and separation on a single substrate, microfluidic systems offer significant advantages such as high sensitivity, speed of analysis, low sample and reagent consumption, and measurement automation and standardization. [1, 2] So far, microfluidic structures are still dominantly produced using photolithography-based techniques. These techniques require multistep stacking and bonding procedures to produce 3D structures. [3, 4] As a direct fabrication technique requiring no masks, femtosecond laser direct writing provides a straightforward approach for high precision, spatially-selective

modification inside transparent materials. [5-10] Recently, we have demonstrated that direct-writing inside porous glass followed by post-annealing enables fabrication of microfluidic channels with lengths much greater than those achievable by conventional femtosecond laser microfabrication techniques, such as the femtosecond laser assisted chemical etching, [11,12] and liquid-assisted femtosecond laser 3D drilling.[13,14] Nevertheless, our previous results, including a square-wave-like microchannel structure [15] and a 3D microfluidic mixer, [16] have not fully examined the capability of this technique for fabricating extremely compact microfluidic systems with long microchannels confined in a small volume. In this contribution, by optimization of the fabrication parameters, we demonstrate fabrication of complex 3D microchannels with a total length of ~6.0 cm in a tiny volume of ~80 nl in glass substrates by

femtosecond laser direct writing. The technique offers great potential for downsizing analytical systems in which long fluidic channels are required, such as electrophoresis microchips, etc. [18-19]

## 2. Experimental

In this experiment, a high-silica porous glass was used as the substrate material for femtosecond laser direct writing. The porous glass samples were obtained by removing the borate phase from phase-separated alkali-borosilicate glass in hot acid solution. The phase-separated alkali-borosilicate glasses were cut to 10 mm × 10 mm × 2 mm coupons and polished before treated in hot acid. The composition of the porous glass is approximately 95.5SiO<sub>2</sub>-4B<sub>2</sub>O<sub>3</sub>-0.5Na<sub>2</sub>O (wt. %). The pores with a mean diameter of ~10 nm occupy 40% volume of the glass and distributed uniformly in the glass to form a 3D connective network in the glass which allows liquid to flow through.

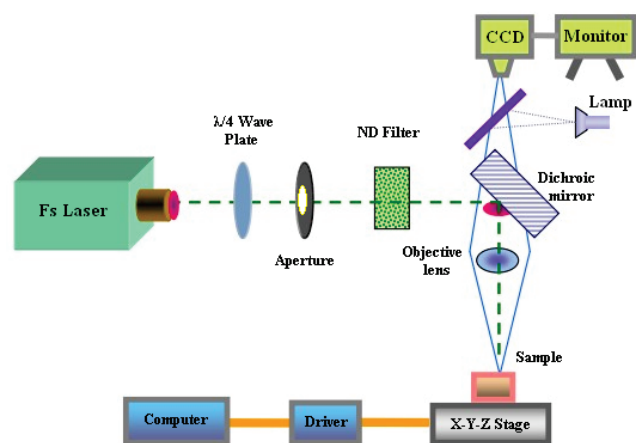


Fig. 1 Schematic of setup for femtosecond laser direct writing

The experiment setup is shown in Fig. 1. A chirped pulse amplification laser system delivers 50 fs laser pulses with a repetition rate of 250 kHz at a center wavelength of 800 nm (Legend USP, Coherent Inc.). A quarter-wave plate is used to generate a circularly polarized laser beam. The initial 8.8 mm diameter beam is trimmed to 5 mm by a circular aperture so as to guarantee a high beam quality. The pulse energy of femtosecond laser is adjusted by a variable density filter. A water-immersed objective lens (100×, NA=1.0) is employed for tightly focusing the femtosecond laser beam into the mesoporous glass sample ~180 μm beneath the sample surface. The sample is translated by a computer-controlled X-Y-Z stage with a

resolution of 1 μm. In this work, the tightly focused high-repetition-rate femtosecond laser pulses are used to generate significant amount of heat and strong shock waves, which can facilitate water circulation and promote the debris removal from the outlet of microchannel. [16-17]

The main fabrication process includes two steps: direct formation of hollow microchannels in a porous glass substrate immersed in water by femtosecond laser ablation and postannealing of the fabricated porous glass sample at ~1150 °C for consolidation of the sample. It is noteworthy that during the laser ablation, clogging sometimes occurred which terminated the transverse drilling of the microfluidic channel. In such a case, we repeatedly scanned the clogged area multiple times until the debris was completely removed. The drilling process can then resume. During the postannealing, the temperature inside the furnace was ramped up to ~1150 °C at a rate of 1 °C /min and held at ~1150 °C for 2 hrs and then naturally air-cooled down to room temperature. The original glass substrate, which was opaque due to scattering by the nanopores, became highly transparent after the postannealing. Since all the pores were collapsed, the volume of the compact substrate would be reduced by ~40% in comparison to that of the porous glass substrate without undergoing the postannealing. As a result, the diameter of the microchannel decreased homogeneously in all three dimensions, whereas the cross sectional shape of the microchannel remains nearly unchanged.

## 3. Dependence of channel diameter on pulse energy

Top view optical micrographs of microfluidic channels embedded in porous glass before post-annealing fabricated at different pulse energies are shown in Fig. 2(a). To investigate the diameter of the microchannel as a function of laser power, eight microchannels were fabricated 180 μm beneath the porous glass surface with different pulse energies of 3, 2, 1.6, 1.2, 0.8, 0.4, 0.36, and 0.32 μJ. All the channels were written with femtosecond laser pulses at a same translation speed of 10 μm /s. Fig. 2(b) shows the cross-sectional view of the cleaved microchannel after post-annealing. The diameters of the microchannels fabricated at these pulse energies, in an order from high energy to low energy, were measured to be 20.82, 12, 11.2,

9.45, 8.7, 6.8, 4.9 and 3.4  $\mu\text{m}$ , respectively. It is clear that the diameter of the microchannel decreases with decreasing pulse energy. Thus, tuning pulse energy of the femtosecond laser can be an efficient approach for controlling the cross sectional size of the microfluidic channel.

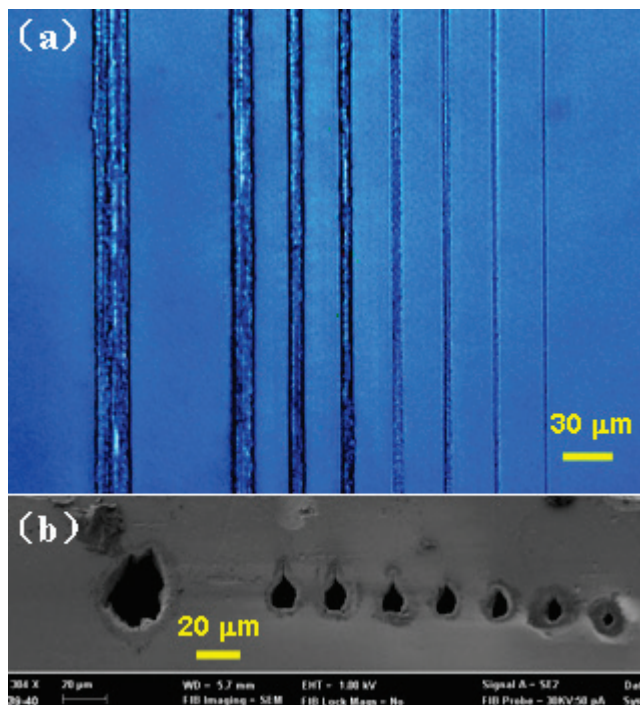


**Fig. 2** (a) Top view optical micrograph of microfluidic channels fabricated in porous glass at different pulse energies. (b) SEM image of the cross-sectional view of the cleaved microchannels after the postannealing.

The microfluidic channels in Fig. 2 show rough inner surfaces which could be caused mainly by two effects: (1) the surface roughness induced by femtosecond laser ablation; and (2) by the re-deposition of debris produced during the fabrication of the channel. In our opinion, the latter effect should influence the surface roughness more strongly, but further experimental investigation is required to clarify this point. We have examined the innerwalls of microchannels fabricated under different laser powers [20]. It seems that the inner surface roughness does not change much with increasing or decreasing laser power. We speculate that this is because that we always use the multiple scan scheme for writing the microchannels, which leads to large diameter of the channels with similar inner surface roughness. Since smooth inner surface is always

required for lab-on-a-chip applications, development of techniques for smoothing the inner surfaces of microfluidic channels fabricated in porous glass is under way.

#### 4. Direct writing of a 6 cm-long 3D microfluidic channel with a two-layer configuration

Many microfluidic applications such as electrophoresis require long channels compactly deployed in a tiny space. Compact microfluidic systems not only reduce the sizes of micro-analysis systems but also promote device performances such as sensitivity. Toward this goal, we fabricated a 3D two-layer microfluidic channel structure in porous glass with a length up to  $\sim 6$  cm. Such a channel length can be sufficient for electrophoresis-based chemical analysis. For example, in Refs. [21-22], the lengths of capillaries are in the range of  $\sim 3$  to  $\sim 5$  cm. A schematic diagram of the 3D microchannel is shown in the Fig. 3(a). Fig. 3(b) shows the top view optical micrographs of the microfluidic channel fabricated in porous glass before post-annealing. The multi-layer microchannel in 3D space was fabricated by translating the sample in a line-by-line and layer-by-layer manner, and the scan of the microfluidic channel started from the lower layer in order to avoid the extra aberration induced by the structures fabricated beforehand in the upper layers. In this case, femtosecond laser pulses with a pulse energy of  $\sim 3.5$   $\mu\text{J}$  were tightly focused into the glass substrate using a water-immersed objective ( $100\times$ , N.A.= 1.0). The microfluidic channel was written at a low translation speed of  $10$   $\mu\text{m/s}$  which can ensure the continuous removal of the debris formed in the microfluidic channel. The significant amount of heat and strong shock waves generated by the femtosecond laser ablation can facilitate water circulation and help to remove the debris from the outlet of the microchannel. The 3D microchannel in Fig. 3(b) has a total length of  $\sim 6.6$  cm, which is compactly folded within a tiny volume of only  $\sim 120$  nl. The dimensions of the 6.6 cm-long channel were measured to be  $\sim 10$   $\mu\text{m}$  in width and  $\sim 12$   $\mu\text{m}$  in height, and the distance between the two layers was  $\sim 30$   $\mu\text{m}$ . The total time for fabricating the 3D microfluidic channel in Fig. 3(b) is  $\sim 3$  hrs. In fact, the length of the microchannel can even be further extended if one would like to spend longer fabrication time.

Fig. 3(c) shows the fluorescence microscope image of

the 3D microchannel filled with a solution of fluorescein under the excitation with a mercury lamp. The confined fluorescent solution gives a proof that the nanopores have all collapsed to form the consolidated substrate. It should be stressed that, since the total volume of the annealed substrate was reduced by  $\sim 40\%$  in comparison to that of the unannealed sample, as a result, the total length was reduced from  $\sim 6.6$  cm to  $\sim 6.0$  cm. The folded microfluidic channel occupies a tiny volume of only  $\sim 80$  nl. To our best knowledge, this is so far the longest 3D microfluidic channel (i. e., corresponding to an aspect ratio of  $\sim 5,000$ ) directly embedded inside a glass substrate by femtosecond laser microprocessing.

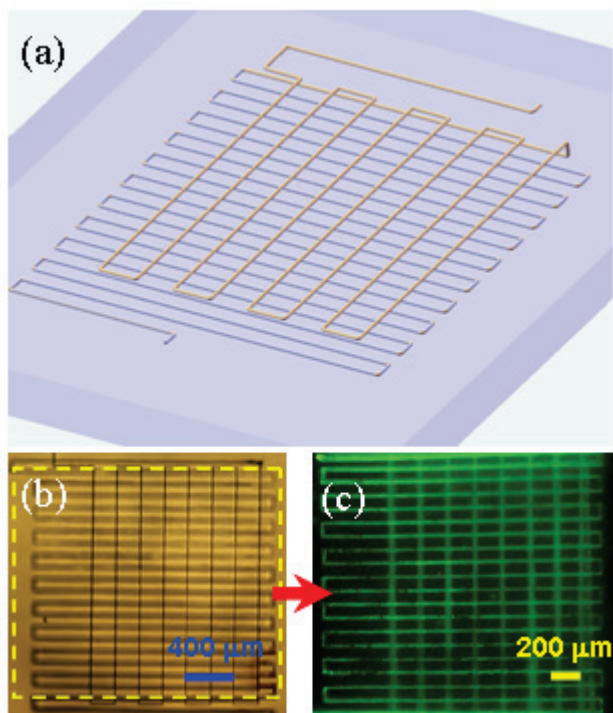


**Fig. 3** (a) Schematic diagrams of the 3D microchannel, and (b) optical micrograph of a 3D microchannel arranged in a compact space before the postannealing of the fabricated sample. (c) The fluorescence microscope image of the 3D microchannel filled with a solution of fluorescein. The volume of the substrate is reduced by  $\sim 39\%$  as a result of the collapse of the nanopores. Only the part inside the yellow box in (b) is shown in (c) for a close-up view.

In general, high irradiation powers are required for producing long microfluidic channels in the porous glass for generating strong shock wave in order to more efficiently remove the debris. In such cases, the diameter

of the channel will increase. On the other hand, debris can also be more efficiently removed by using the multiple scan scheme for the laser writing instead of using a single scan scheme. We have seen in our experiment that if sometimes a clog occurs due to the deposition of the ablation debris in the microfluidic channel, then no bubbles can come out from the channel (due to the clog) even if we continue the writing process in the porous glass. However, in such a case, if we could remove the deposited debris by performing multiple scans around the clogging area, the length of microfluidic channel can be easily extended afterwards. Thus, some important parameters, such as writing speed, laser power, numbers of scans, focal conditions, etc., should be carefully optimized for creating microfluidic channels of long lengths but small diameters.

An interesting question is that, by femtosecond laser direct writing in the porous glass, will it be possible to produce very thin channels, e. g., channels with diameters less than  $1\ \mu\text{m}$  by use of the well-known threshold effect [23, 24]. In our experiment, we have seen that we can reduce the channel diameter to  $\sim 1\ \mu\text{m}$  whereas still maintain a nearly circular cross sectional shape of the channel. However, in such cases, the channels are shorter than the thick ones. More interestingly, recently we have shown that nanofluidic channels with a width of  $\sim 40$  nm and a height of  $\sim 1\ \mu\text{m}$  can be readily achieved by combining the threshold effect and nanograting effect [25]. For a nanofluidic channel with a width of  $\sim 40$  nm, its length can reach  $\sim 50\ \mu\text{m}$ , which is sufficient for single molecule analysis applications [26]. The quantitative dependence of the maximum channel length on the channel diameter will be investigated in great detail in our future work.

## 5. Conclusion

In conclusion, we have shown that long microchannels with multi-layer configurations in 3D space can be fabricated in glass substrates within a small volume by femtosecond laser direct writing. We demonstrate a 3D microfluidic channel with a length up to  $\sim 6.0$  cm in a tiny volume of  $\sim 80$  nl embedded in glass. The device can allow for downsizing lab-on-a-chip applications which require long channel lengths, such as dielectrophoretic separation of biomolecules and so on.

## Acknowledgements

This work is supported by National Basic Research Program of China (Grant No. 2011CB808102) and National Natural Science Foundation of China (Grant Nos. 10974213, 60825406, 61275205 and 11204332).

## References

- [1] G. M. Whitesides, *Nature* 442 (2006): 368-373.
- [2] A. Manz, N. Graber, and H. M. Widmer, *Sens. Actuators B* 1 (1990): 244-248.
- [3] M. S. Giridhar, K. Seong, A. Schülzgen, P. Khulbe, N. Peyghambarian, and M. Mansuripur, *Appl. Opt.* 43 (2004) 4584-4589.
- [4] B. H. Jo, L. M. Van Lerberghe, K. M. Motsegood, and D. J. Beebe, *J. Microelectromech Syst.* 9 (2000): 76-81.
- [5] Y. Cheng, K. Sugioka, K. Midorikawa, M. Masuda, K. Toyoda, M. Kawachi, and K. Shihoyama, *Opt. Lett.* 28 (2003): 1144-1146.
- [6] C. Lee, T. Chang, S. Wang, C. Chien, and C. Cheng, *Biomicrofluidics* 4 (2010): 046502-046506.
- [7] F. He, Y. Cheng, Z. Z. Xu, Y. Liao, J. Xu, H. Y. Sun, C. Wang, Z. H. Zhou, K. Sugioka, K. Midorikawa, Y. Xu, and X. Chen, *Opt. Lett.* 35 (2010): 282-284.
- [8] J. Cheng, C. Wei, K. Hsu, and T. Young, *Sens. Actuators B: Chem* 99 (2004): 186-196.
- [9] Y. Cheng, K. Sugioka, and K. Midorikawa, *Appl. Surf. Sci.* 248 (2005): 172-176.
- [10] K. Sugioka, Y. Cheng, and K. Midorikawa, *Appl. Phys. A* 81 (2005): 1-10.
- [11] K. Sugioka, Y. Cheng, *Lab Chip* 12 (2012): 3576-3589.
- [12] A. Marcinkevicius, S. Juodkazis, M. Watanabe, M. Miwa, S. Matsuo, H. Misawa and J. Nishii, *Opt. Lett.* 26 (2001): 277-279.
- [13] R. An, Y. Li, Y. Dou, D. Liu, H. Yang, and Q. Gong, *Appl. Phys. A* 83 (2006): 27-29.
- [14] D. J. Hwang, T. Y. Choi, and C. P. Grigoropoulos, *Appl. Phys. A* 79 (2004): 605-612.
- [15] Y. Liao, Y. F. Ju, L. Zhang, F. He, Q. Zhang, Y. L. Shen, D. P. Chen, Y. Cheng, Z. Z. Xu, K. Sugioka, and K. Midorikawa, *Opt. Lett.* 35 (2010): 3225-3227.
- [16] Y. Liao, J. X. Song, E. Li, Y. Luo, Y. L. Shen, D. P. Chen, Y. Cheng, Z. Z. Xu, K. Sugioka, and K. Midorikawa, *Lab Chip* 12 (2012): 746-749.
- [17] C. N. Liu, Y. Liao, F. He, Y. L. Shen, D. P. Chen, Y. Cheng, Z. Z. Xu, K. Sugioka, and K. Midorikawa, *Opt. Express* 20 (2012): 4291-4296.
- [18] D. J. Harrison, K. Fluri, K. Seiler, Z. H. Fan, C. S. Effenhäuser, and M. Andreas, *Science* 261 (1993): 895-897.
- [19] A. T. Woolley and R. A. Mathies, *Proc Natl Acad Sci U S A* 91 (1994): 11348-11352.
- [20] Y. F. Ju, Y. Liao, L. Zhang, Y. L. Sheng, Q. Zhang, D. P. Chen, Y. Cheng, Z. Z. Xu, K. Sugioka, K. Midorikawa, *Microfluid Nanofluid* 11 (2011): 111-117.
- [21] J. J. Zhu, X. C. Xuan, *Journal of Colloid and Interface Science* 340 (2009): 285-290
- [22] A. L. Garcia, L. K. Ista, D. N. Petsev, M. J. O'Brien, P. Bisong, A. A. Mammoli, S. R. J. Brueck, G. P. Lopez, *Lab Chip* 11 (2005): 1271-1276.
- [23] S. Kawata, H. B. Sun, T. Tanaka and K. Takada, *Nature* 412 (2001): 697-698.
- [24] A. P. Joglekar, H. H. Liu, E. Meyhöfer, G. Mourou, and A. J. Hunt, *Proc Natl Acad Sci U S A* 101 (2004): 5856-5861.
- [25] Y. Liao, Y. L. Shen, L. L. Qiao, D. P. Chen, Y. Cheng, K. Sugioka, and K. Midorikawa, *Opt. Lett.* 38 (2013): 187-189.
- [26] Y. Liao, Y. Cheng, C. N. Liu, J. X. Song, F. He, Y. L. Shen, D. P. Chen, Z. Z. Xu, Z. C. Fan, X. B. Wei, K. Sugioka and K. Midorikawa, *Lab Chip* 13 (2013): 1626-1631.

(Received: February 4, 2013, Accepted: May 23, 2013)